Rainfall Induced Landslide Detection using Persistent Scatterer Interferometry

Annu Kumari*, Dharmendra Singh, & Sultan Singh

Haryana Application Centre Hisar, India
*Corresponding Author's email: dsbaghel0184@gmail.com

Abstract

Landslides are the downhill movement of a mass of rock, debris, or subsurface material caused by a variety of external and internal stresses such as severe rainfall, earthquake shaking, change in water level, storm waves, or rapid stream erosion and claim many lives and cause significant economic damages. Rainfall, soil, and slope all play essential roles in rainfall-induced landslide (RIL) formation. The present study is done for the identification of RIL in North Haryana using Sentinel-1 SLC product from January to July (months show heavy rainfall). Persistent (Permanent) Scatterer Interferometry (PSI or PsINSAR) technique was used which is an advanced Differential Interferometry Synthetic Aperture Radar (DInSAR) technique that can monitor and track surface displacements throughout a defined time period. In the PSI technique, the Permanent Scatterer (PS) selection method is based on phase characteristics, and for phase selection Amplitude Dispersion Index (ADI) is used. The high ADI values show unstable PS (most likely water, agriculture area) while stable PS have low ADI values (man-made features, Outcropping area). For the present study, a threshold value of ADI i.e., =<0.4 is used to segregate and analyse the stable features, which might have been affected by RIL. The average Phase displacement was observed to be -3mm to -2mm, with a velocity of ≃3 cm (for specific part with low ADI values), which show change on the surface probably due to landslide. For the verification of these PS points high resolution PlanetScope images (≃3.5×3.5 m) of pre-event (15 April 2023) and post-event (20 July 2023) were taken which showed landslide signature. Some areas of the Ghaggar river have shown high displacement and indicate landslides probably due to overflow of water which might have broken river banks. The analysis is beneficial for the detection of actual landslide locations which is an essential requirement for disaster management.

Key Words SAR, Interferometry, Disaster management, Sentinel-1, Haryana.

Introduction

Landslides are the dynamic event of downward movement of slope-forming materials composed of natural rock, soils, debris, manmade fills, and subsurface material (Cruden, 1991; Dai et al., 2001; Varnes, 1958). The mass movement can be caused by a variety of external and internal stresses such as excess rainfall, earthquake shaking, change in water level, storm waves, or rapid stream erosion and claim many lives and cause significant economic damages (Cruden, 1991). Rainfall-induced landslides (RILs) are natural disasters that cause a high number of causalities and economic damage each year (Dai et al., 2001; Toribio et al., 2022). According to Toribio et al. (2022) rainfall, soil, and slope all play essential roles in RILs development formation.

RILs detection and monitoring are essential for managing and mitigating the risk of landslides. In order to detect and monitor landslides, remote-sensing techniques such as Earth observation from space, laser scanning, and ground-based interferometry provide a systematic and synoptic view across many spatiotemporal scales. Ground-based remote-

sensing applications cover a small but precise area so in this way their uses are limited. In contrast, Earth observation satellites can observe a large area in near real-time. Synthetic Aperture Radar (SAR)-based satellites continuously provide radar images of the Earth's surface without being influenced by atmospheric conditions (Oliver, 1991). SAR sends microwave signals and receives them back from the surface, which is known as backscatter. Backscatter contains phase and amplitude in a complex matrix. The phase is then used to compute the distance between the sensor and the target, while the amplitude is used to calculate the amount of signal sent that returns to the sensor. Interferometry is a method that gives an analysis using SAR data, which is also called InSAR (Interferometry Synthetic Aperture Radar). InSAR measures the distance between the sensor and the target using the phase information acquired by the sensor. The change between the phase of two Line of Sight (each captured across different time periods) of the same target is computed as a change in surface topography. In other words, it evaluates changes in land surface topography using at least two radar images of the same object obtained by the sensor with geometry information. The measurements obtained from InSAR are accurate up to millimetre or centimetre level and can be used to identify areas of deformation from events like volcanic eruptions, earthquakes, and landslides.

Wempen, 2020 suggested that Differential Interferometric Synthetic Aperture Radar (DInSAR) is an InSAR method that can be used to measure the displacement of the Earth's surface. It uses two radar images to measure centimetre-scale surface displacements. However, DInSAR has some limitations such as a high temporal difference between two observations, which affects the analysis of phase measurement. In addition, atmospheric parameters can also influence the measurement of interferograms. So, an improved version of InSAR was proposed by (Hooper et al., 2004) - Persistent (Permanent) Scatterer Interferometry (PSI) or PsINSAR which is an advanced DInSAR technique that can monitor and track surface displacements over time. Hooper et al., 2004 and Jia et al., 2016 suggested that PSI is a time series analysis of multiple radar images. This technique is based on permanent pixels and is also called permanent scatterer which means only those scatterers are used for analysis which are stable or permanent pixels like manmade features. The atmospheric effects can be filtered out and the temporal and geometrical decorrelation can be eliminated by using permanent scatterers.

Recently, many studies have focused on the applications of PSInSAR technique (Awasthi et al., 2022; Beladam et al., 2019; Besoya et al., 2021; Correa-Munoz et al., 2019) for the deformation monitoring of the Earth's surface and detecting hazards such as landslides. Hussain et al., 2019 utilize it for validation of ground truth, drone-based data for landslide. However, the RILs studies using the PSInSAR technique are deficient, especially in Haryana's northern hilly regions. The goal of the present study is to monitor recent rainfall-induced landslides using the PsINSAR technique for the Panchkula district of Haryana. In order to understand the potentiality of PsINSAR we generated a detailed methodology of StaMPS (Delgado Blasco et al., 2019)-based PsINSAR technique. To test the methodology Sentinel-1 SLC product from January to July of 2023 was analysed. The present study consists of five sections. Section 1 consists of the introduction of the study introduction followed by section 2 which presents details about the study area, while section 3 includes an explanation of the database and methodology. Section 4 presents the results and discussion, followed by section 5, which gives the conclusion of the study.

Materials and Methods

Study area: This study focuses on the only mountainous region of Northern Haryana from where the Ghaggar river enters the plains from the hills of the Panchkula district. Morni Hills is considered the highest point of the district as well as of Haryana. Panchkula is a combination of the words panch (five) and kul (canal), which translates to "a city of five canals" and is situated between 30° 26′–30° 55′ North and 76° 46′–77° 10′ East. Ghaggar is the only perennial river that is also quite shallow outside of the monsoon season. The slope of the area trends from northeast to southwest, and the majority of the rivers/streams are rain-fed torrents that flow down and deposit a lot of gravel and stones in their beds. Panchkula is situated near the Himalayan fault zones, which have experienced moderate to severe earthquakes in the recent past. The topography of the district is carved into sharp slopes by the many ephemeral streams that descend to the outer slopes of the Siwalik Hills, spreading many gravel stones in the beds of these streams. The district's average annual rainfall is ~1057 mm, with the Siwalik Hills occupying the north and northeast part of the district of Panchkula, reaching heights of up to 950 m AMSL (Above Mean Sea Level) (Kanga et al.,2022). The rainfall is mostly received in the monsoon season however, the district also receives winter rains (December and January) from the western disturbance.

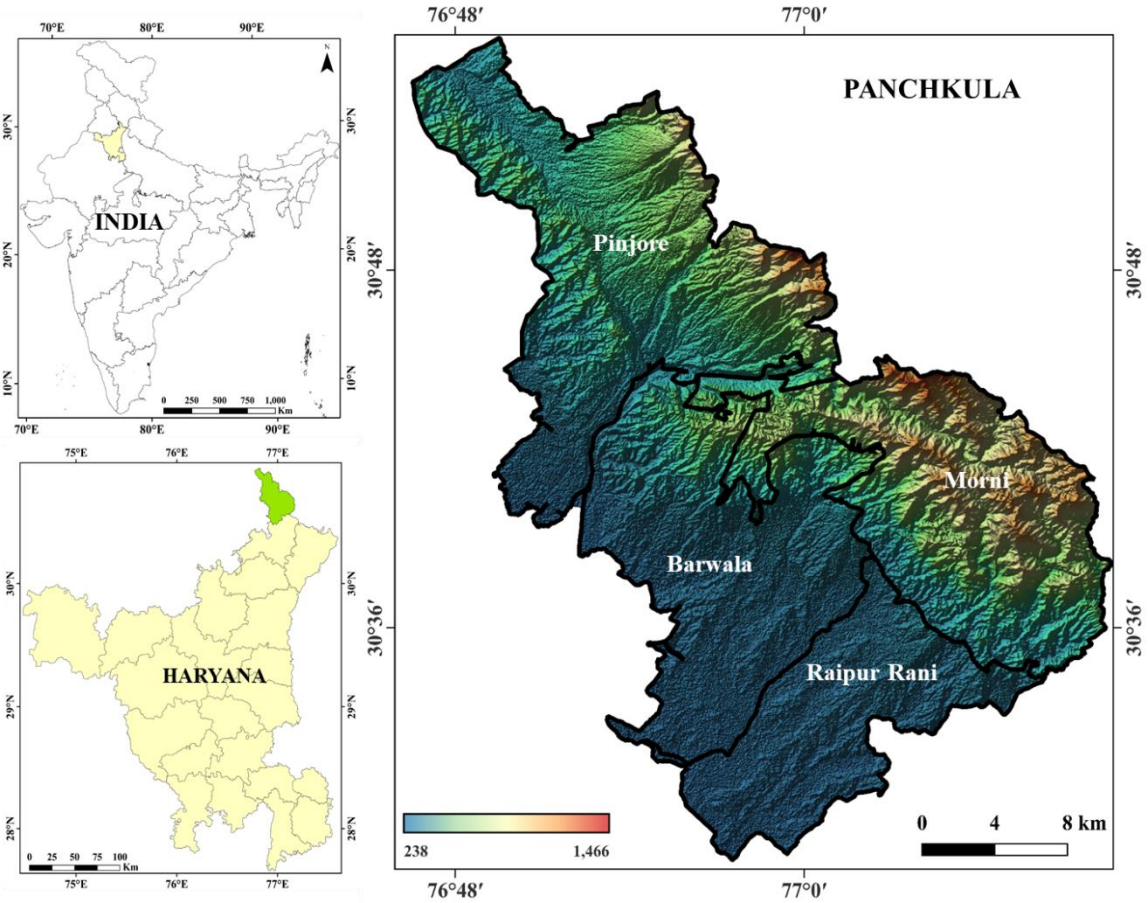

Fig. 1 Study area map showing the location of Panchkula district and elevation of study area.

Datasets: Sentinel-1A data from Sentinel-1 mission has been used for the current study. Sentinel-1A is a satellite sensor operated by the European Space Agency. Sentinel-1A launched on 3 April 2014, and Sentinel-1B debuted on 22 April 2016. Sentinel-1A is still operational; however, Sentinel-1B has been decommissioned since December 2, 2021. Sentinel-1A is in a near-polar, sun-synchronous orbit with a 12-day repeat cycle and a total of 175 orbits each cycle. As previously mentioned, the Sentinel-1 IW (Interferometry Wide swath) SLC (Single Look Complex) product from January to July of 2023 has been analysed for the study. A set of 13 images (Table 1) from Sentinel-1A was obtained from the Copernicus Open Access Hub.

The images were acquired along descending pass and a master image (13 May 2023) was also chosen based on the minimization of the perpendicular baseline and temporal baseline. For the validation purpose average rainfall data (from January to July of 2023) was also used from CHIRPS (Climate Hazards Group InferaRed Precipitation with Station data) that provide rainfall data on a daily basis. Visual validation was also done using high-resolution PlanetScope images (≃3.5×3.5 m) of pre-event (15 April 2023) and post-event (20 July 2023).

Table 1. List of Sentinel-1A IW SLC images.

Sentinel-1A SLC Product Name	Date Of Acquisition	Pass
S1A_IW_SLC__1SDV_20230101T005204_20230101T005231_046583_059524_8F9F	01-01-2023	Descending
S1A_IW_SLC__1SDV_20230125T005203_20230125T005230_046933_05A0F3_C083	25-01-2023	Descending
S1A_IW_SLC__1SDV_20230218T005202_20230218T005229_047283_05ACB0_E952	18-02-2023	Descending
S1A_IW_SLC__1SDV_20230314T005202_20230314T005229_047633_05B88A_8565	14-03-2023	Descending
S1A_IW_SLC__1SDV_20230407T005202_20230407T005229_047983_05C455_9F81	07-04-2023	Descending
S1A_IW_SLC__1SDV_20230501T005203_20230501T005230_048333_05D01F_80DF	01-05-2023	Descending
S1A_IW_SLC__1SDV_20230513T005204_20230513T005231_048508_05D5C0_D45F	13-05-2023	Descending
S1A_IW_SLC__1SDV_20230525T005204_20230525T005231_048683_05DAF1_D8CC	25-05-2023	Descending
S1A_IW_SLC__1SDV_20230606T005205_20230606T005232_048858_05E029_0917	06-06-2023	Descending
S1A_IW_SLC__1SDV_20230618T005206_20230618T005233_049033_05E580_A682	18-06-2023	Descending
S1A_IW_SLC__1SDV_20230630T005206_20230630T005233_049208_05EACB_5A15	30-06-2023	Descending
S1A_IW_SLC__1SDV_20230724T005208_20230724T005235_049558_05F58F_1A8E	24-07-2023	Descending

Methodology: The methodology is divided into two major parts, the first is to generate an interferogram for each image with the master image and the second is performing phase analysis. This first step also consists of multiple preprocessing steps such as Apply orbit file computing geometric shift between slave and master image, then split to reduce the size of the image, and finally coregistration of each pair (slave and master image) with enhanced spectral diversity and back geocoding. After the generation of interferograms, the topographic phase has been removed. This step requires a DEM (Digital Elevation Model). In this case, SRTM DEM was used for this purpose. Before moving on second step stable pixels or stable amplitude are calculated using ADI (Amplitude Dispersion Index) (Jia et al., 2016; Serco Italia SPA, 2020). The ADI is a measure that describes amplitude stability and is used to preselect pixels, reducing the amount of pixels needed in the phase analysis.

$$\text{ADI} = \sigma A / \mu A$$

Where σA is the standard deviation and μA represents the mean of a set of amplitude values.

For this study 0.40 ADI is used for calculating stable pixels because man-made features and bedrock outcroppings are permanent features that also have stable pixels or stable amplitude, their ADI range is indicated to be between 0.40-0.42 (Jia et al., 2016; Serco Italia SPA, 2020). If the threshold of ADI is increased, more pixels are chosen for phase analysis. Surfaces with unstable amplitudes, such as water and plants, have higher ADI values than bedrock outcroppings or man-made structures.

The second step concerns the correction of phase information, coherence estimation, and atmospheric correction of PS (Permanent Scatterer) points. PS (Permanent Scatterer) points in the interferogram, which provides phase values that measure displacement or change in LOS (Line of Sight) between 0 to 2π for each cycle of wavelength. So, converting them to real values and removing the ambiguity, we performed phase unwrapping with the help of snaphu. Following this, we obtained velocity for deformation of LOS/per year in mm or rate of displacement per year and phase information in mm from each image which was plotted on StaMPS visualiser (Figure 3).

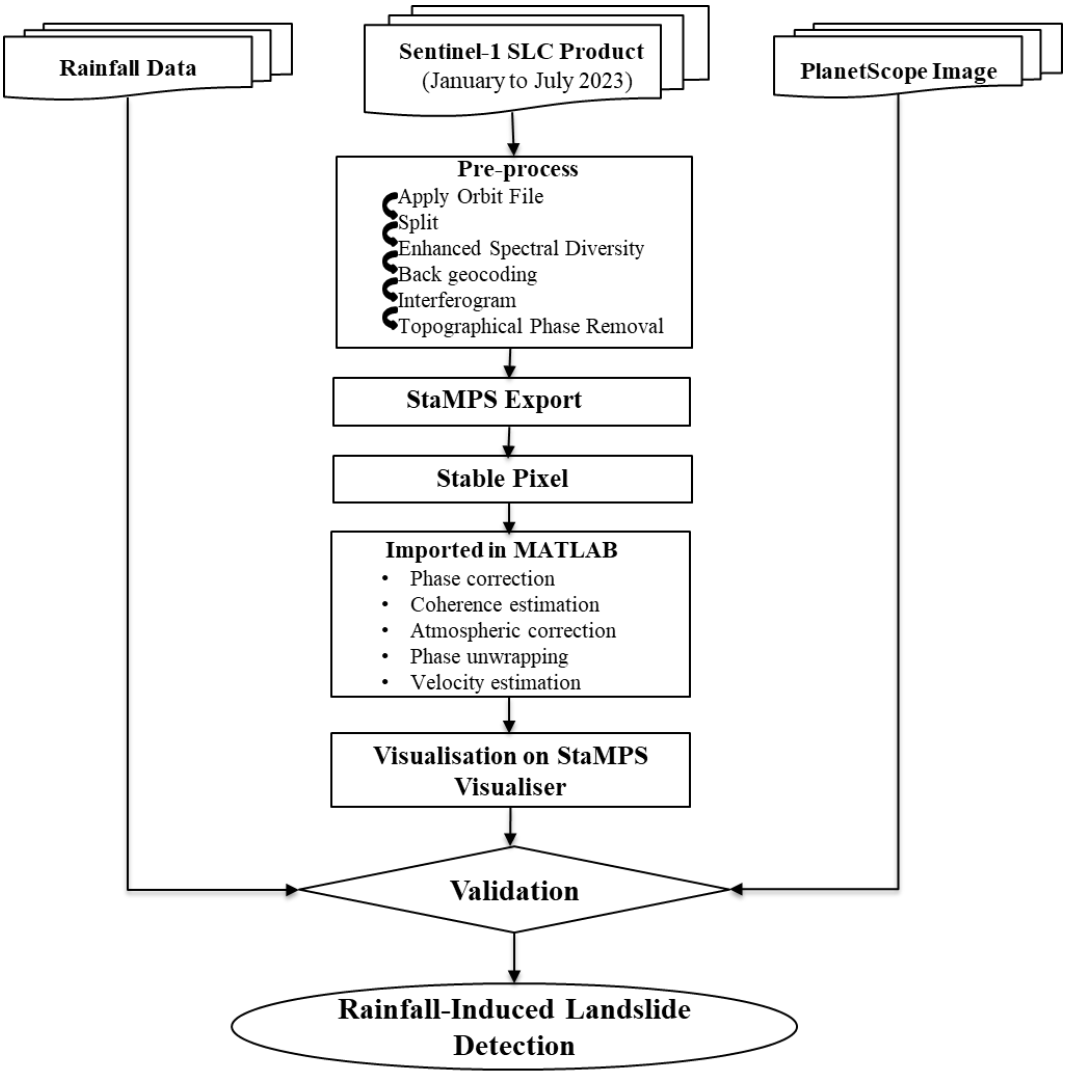

Fig. 2. Flow chart of StaMPS-based PSInSAR methodology.

To validate the results of the study, average rainfall was calculated and plotted with the phase value of a particular PS point (marked in Figure 4b). In addition, we also used PlanetScope images as supporting evidence for the RILs due to their high temporal and high-resolution capability.

Results and Discussions

STAMPS-based PsINSAR methodology has been analysed to monitor the recent RILs that have occurred in the Panchkula district. For the purpose of analysis, a small number of PS points were taken which fall within a 10 km radius from the center of Panchkula city (Figure 3). In order to represent these PS points on StaMPS Visualiser (Figure 3), PS points were plotted on a leaflet layer to understand the location of each PS. The observed velocity of LOS ranges between -60 mm to 60 mm per year which suggests the rate of displacement is occurring per year between -6 cm to 6 cm. In Figure 3a, the deep red and red points show a high velocity of land deformation, which translates to increased distance between the sensor and the target while blue points show decreased distance between the sensor and the target, whereas yellow points indicate no change between sensor and target.

Fig.4a shows an area (marked in red circle) that has a large number of deep red and red points in contrast to other areas. A magnified view of Figure 4a (as shown in Figure 4b) shows a slope where the Ghaggar river flows in the upper part and a road is visible towards the Morni Hills in the lower part in the base map. The deep red point located in this area provides insight into recent changes the surface has faced, which may point to a landslide as the particular location was on a hilly slope. For a detailed analysis of phase difference, each point was observed from the red circle (Figure 4a). It was found that the phase has an average change of approximately 2-4 mm downwards from January to July of 2023. However, in the month of July 2023 when a sudden heavy rainfall occurred the phase also drastically reduced. In this regard, -28 mm was observed from a particular point of Figure 4b that has been marked by a yellow circle.

The results prove that the topography of the study area has changed. However, it is not clear if the cause was due to rainfall or not. In order to verify this, rainfall data was also used (Figure 5). The phase value of a particular point and average rainfall were plotted together to find their relationship. Results reveal that whenever heavy rainfall takes place phase difference also changes. However, a drastic fall can also be observed in the phase around 6th July, and around that time rainfall was also high, which shows the increased phase difference is directly related to rainfall.

In order to further validate our results PlanetScope satellite imagery of two different dates was acquired i.e. one of 15th April 2023 and the other of 20th July 2023 (Figure 6). Figure 6a shows that Ghaggar River has a very low water level on the other hand Figure 6b shows that the water level has increased in the river which has also breached the river bank. Possible causes could be due to sudden heavy rainfall in that area. A large green patch in Figure 6a has deformed in Figure 6b indicating that heavy water flow outside the broken river bank has forced surface material downhill which resulted in a landslide.

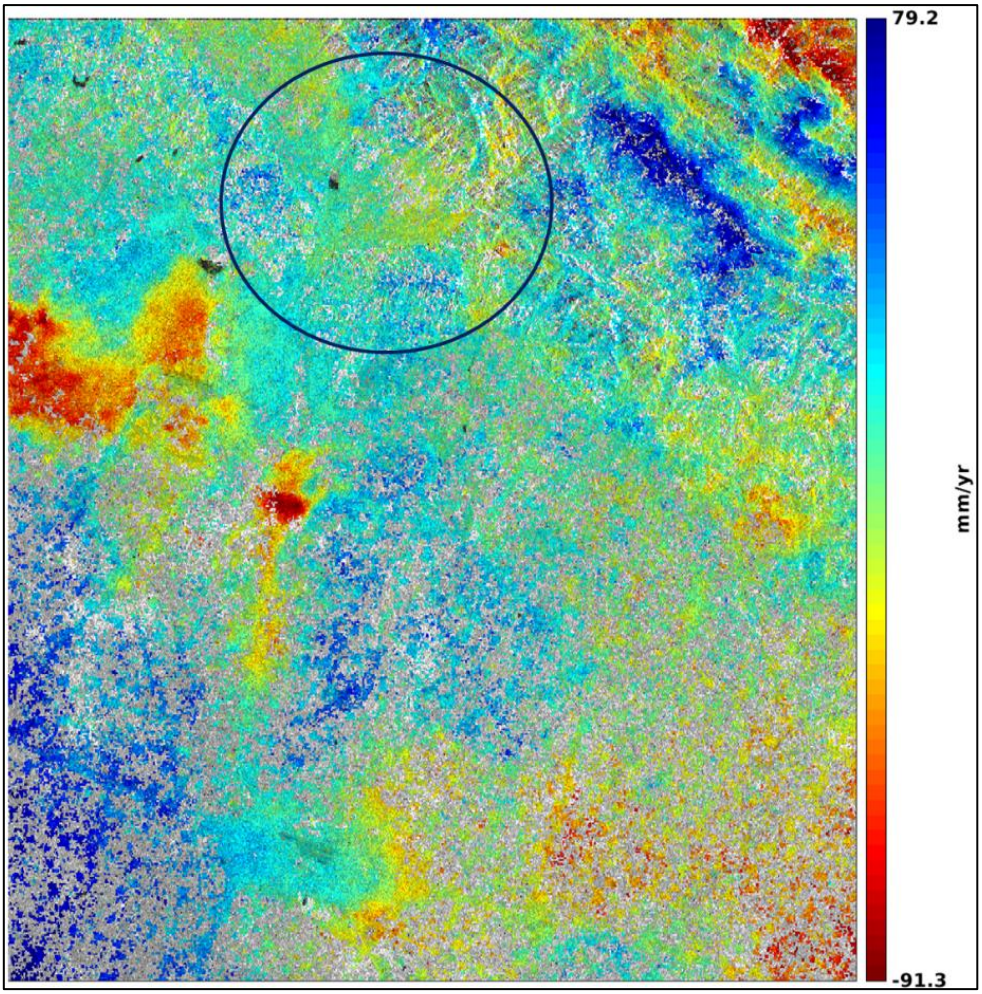

Fig. 3 The observed velocity of LOS in mm/yr.

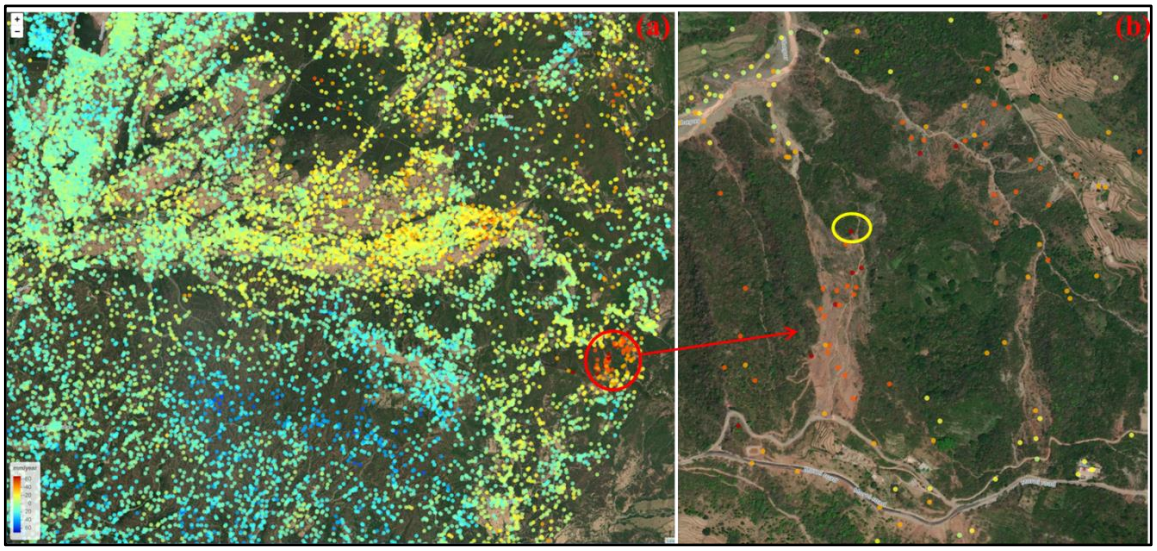

Fig. 4 Permanent Scatterers plotted on StaMPS visualizer**.**

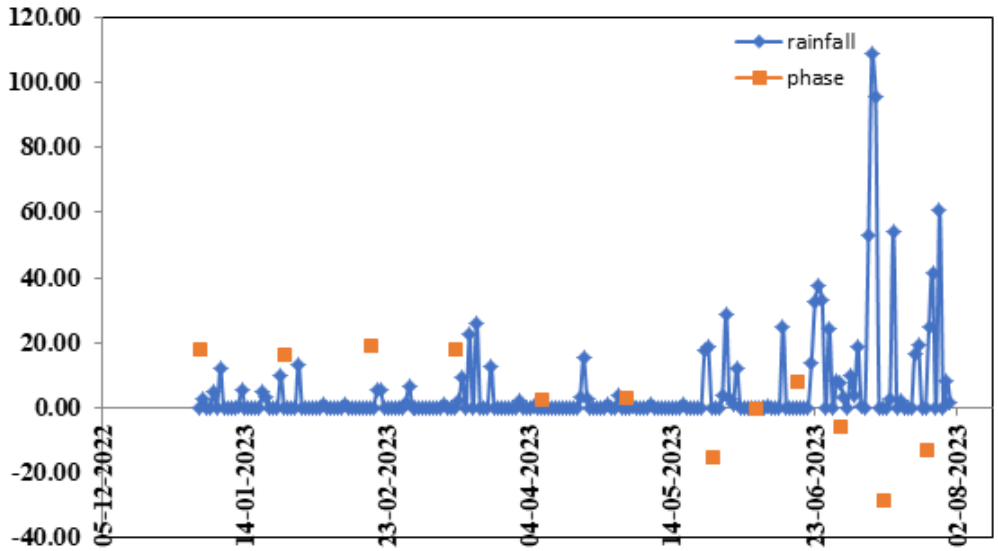

Fig. 5 Plot showing average rainfall and phase displacement.

After the observation of both PlanetScope images (Figure 6) and the line plot shown in (Figure 5), we can say that a landslide had occurred due to a heavy flow of water which was caused by a sudden heavy rainfall in the Panchkula district. This event has been well captured by PSInSAR-based analysis (Figure 4).

Fig. 6 PlanetScope image of landslide (a) 15th April 2023 (b) 20th July 2023.

Conclusions

In this present study, we aimed to evaluate the PsINSAR technique for the identification of rainfall-induced landslides (RILs) in the Panchkula district of Haryana. The analysis of the velocity of LOS and phase of each image helped identify possible RILs, which proves that PSInSAR can be used for RILs as well as various types of landslides. Although we found that the PSInSAR technique can be used for detecting and monitoring landslides as well as land

formation, it is important to note that PSInSAR is a time-series analysis technique, which requires a large database to maintain high accuracy. However, this procedure can be more reliable after using a supporting database which enables us to find the relationship between rainfall and landslides. Hence, StaMPS-based PSInSAR is a reliable method for landslide detection.

Acknowledgments

The work was done at the HARSAC Node Gurugram Lab. We wish to express our sincere appreciation for the generous support received from the organization. We would like to gratefully acknowledge Copernicus Open Data Access, CHIRPS, and PlanetScope for providing a reliable database. We are very thankful to ESA's training program for understanding the importance of Sentinel-1A products and procedures. Also, thanks to Dr. Subhadyouti Bose, Post-Doctoral Fellow, Physical Research Laboratory, Ahmedabad, for support and assistance.

References

1. Awasthi, S., Jain, K., Mishra, V., & Kumar, A. (2022). An approach for multidimensional land subsidence velocity estimation using time-series Sentinel-1 SAR datasets by applying persistent scatterer interferometry technique. Geocarto International, 37(9), 2647-2678. https://doi.org/10.1080/10106049.2020.1831624.
2. Beladam, O., Balz, T., Mohamadi, B., & Abdalhak, M. (2019). Using ps-insar with sentinel-1 images for deformation monitoring in northeast Algeria. Geosciences, 9(7), 315. https://doi.org/10.3390/geosciences9070315.
3. Besoya, M., Govil, H., &Bhaumik, P. (2021). A review on surface deformation evaluation using multitemporal SAR interferometry techniques. Spatial Information Research, 29, 267-280. https://doi.org/10.1007/s41324-020-00344-8
4. Bischoff, C. A., Ferretti, A., Novali, F., Uttini, A., Giannico, C., &Meloni, F. (2020). Nationwide deformation monitoring with SqueeSAR® using Sentinel-1 data. Proceedings of the International Association of Hydrological Sciences, 382, 31-37. https://doi.org/10.5194/piahs-382-31-2020
5. Bonì, R., Meisina, C., Perotti, C., &Fenaroli, F. (2015). PSI-based methodology to land subsidence mechanism recognition. Proceedings of the International Association of Hydrological Sciences, 372(372), 357-360. https://doi.org/10.5194/piahs-372-357-2015
6. Chen, C. W., & Zebker, H. A. (2002). Phase unwrapping for large SAR interferograms: Statistical segmentation and generalized network models. IEEE Transactions on Geoscience and Remote Sensing, 40(8), 1709-1719.
7. Cruden, D. (1991). A simple definition of a landslide. Bulletin of Engineering Geology & the Environment, 43(1).
8. Crosetto, M., Monserrat, O., Cuevas-González, M., Devanthéry, N., &Crippa, B. (2016). Persistent scatterer interferometry: A review. ISPRS Journal of Photogrammetry and Remote Sensing, 115, 78-89. https://doi.org/10.1016/j.isprsjprs.2015.10.011
9. Correa-Munoz, N. A., Tansey, K., & Murillo-Feo, C. A. (2019). Effect of a DEM in the estimation of coherence and unwrapped phase InSAR for landslides detection. In Geotechnical Engineering in the XXI Century: Lessons learned and future challenges (pp. 1693-1700). IOS Press.
10. Dai, F. C., Lee, C. F., & Ngai, Y. Y. (2002). Landslide risk assessment and management: an overview. Engineering geology, 64(1), 65-87.
11. Delgado Blasco, J. M., Foumelis, M., Stewart, C., & Hooper, A. (2019). Measuring urban subsidence in the Rome metropolitan area (Italy) with Sentinel-1 SNAP-StaMPS persistent scatterer interferometry. *Remote Sensing*, *11*(2), 129.
12. Fustos-Toribio, I., Manque-Roa, N., Vásquez Antipan, D., Hermosilla Sotomayor, M., & Letelier Gonzalez, V. (2022). Rainfall-induced landslide early warning system based on corrected mesoscale numerical models: an application for the southern Andes. Natural Hazards and Earth System Sciences, 22(6), 2169-2183.
13. Hooper, A., Zebker, H., Segall, P., & Kampes, B. (2004). A new method for measuring deformation on volcanoes and other natural terrains using InSAR persistent scatterers. Geophysical research letters, 31(23).
14. Hussain, M.A.; Chen, Z.; Wang, R.; Shoaib, M. PS-InSAR-Based Validated Landslide Susceptibility Mapping along Karakorum Highway, Pakistan. *Remote Sens.* **2021**, *13*, 4129. https://doi.org/10.3390/rs13204129

15. Jia, H., & Liu, L. (2016). A technical review on persistent scatterer interferometry. *Journal of Modern Transportation*, *24*, 153-158. https://doi.org/10.3390/rs13204129
16. Kanga, S., Singh, S. K., Meraj, G., Kumar, A., Parveen, R., Kranjčić, N., & Đurin, B. (2022). Assessment of the impact of urbanization on geoenvironmental settings using geospatial techniques: a study of Panchkula District, Haryana. *Geographies*, *2*(1), 1-10. https://doi.org/10.3390/geographies2010001
17. Oliver, C. J. (1991). Information from SAR images. *Journal of Physics D: Applied Physics*, *24*(9), 1493.
18. Wempen, Jessica M. "Application of DInSAR for short period monitoring of initial subsidence due to long wall mining in the mountain west United States." *International Journal of Mining Science and Technology* 30, no. 1 (2020): 33-37. https://doi.org/10.1016/j.ijmst.2019.12.011
19. Serco Italia SPA (2020). SNAP2StaMPS: Data preparation for StaMPS PSI processing with SNAP - Mexico City 2020 (version 1.1).
20. Serco Italia SPA (2020). StaMPS: Persistent Scatterer Interferometry Processing - Mexico City 2021 (version 1.1).
21. Varnes, D. J. (1958). Landslide types and processes. *Landslides and engineering practice*, *24*, 20-47.

Citation

Kumari, A., Singh, D., Singh, S. (2024). Rainfall Induced Landslide Detection using Persistent Scatterer Interferometry. In: Dandabathula, G., Bera, A.K., Rao, S.S., Srivastav, S.K. (Eds.), Proceedings of the 43rd INCA International Conference, Jodhpur, 06–08 November 2023, pp. 322–331, ISBN 978-93-341-2277-0.

A Comparative Assessment of Ground Water Resources using GRACE and Ground Data in Highly Populated Regions of Haryana, India